

# ABC and ABAB block copolymers by electrochemically controlled ring-opening polymerization

Zachary C. Hern, Stephanie M. Quan,<sup>§</sup> Ruxi Dai, Amy Lai, Yihang Wang,<sup>†</sup> Chong Liu,<sup>\*</sup> Paula L. Diaconescu<sup>\*</sup>

Department of Chemistry and Biochemistry, University of California Los Angeles. Los Angeles, California 90095-1569, United States

**ABSTRACT:** An electrochemically controlled synthesis of multiblock copolymers by alternating the redox states of (salfan)Zr(O<sup>*t*</sup>Bu)<sub>2</sub> (salfan = 1,1'-di(2-*tert*-butyl-6-N-methylmethylenephenoxy)ferrocene) is reported. Aided by electrochemistry with a glassy carbon working electrode, an *in situ* potential switch alters the catalyst's oxidation state and its subsequent monomer (L-lactide, β-butyrolactone, or cyclohexene oxide) selectivity in one pot. Various multiblock copolymers were prepared, including an ABAB tetrablock copolymer, poly(cyclohexene oxide-*b*-lactide-*b*-cyclohexene oxide-*b*-lactide), and an ABC triblock copolymer, poly(hydroxybutyrate-*b*-cyclohexene oxide-*b*-lactide). The polymers produced using this technique are similar to those produced via a chemical redox reagent method, displaying moderately narrow dispersities (1.1 – 1.5) and molecular weights ranging from 7 to 26 kDa.

## INTRODUCTION

Through billions of years of evolution, Nature has evolved a sophisticated machinery to produce biopolymers with precise sequence control. This level of precision has inspired chemists to discover tools and methodologies to control the primary structure of synthetic polymers<sup>1-6</sup> such as controlled radical polymerization<sup>7-9</sup> and switchable catalysis.<sup>10-17</sup> Switchable catalysis employs a single precursor capable of accessing multiple, distinct catalytically active states by employing external triggers. These states can display different reactivity rates for the same monomer or exhibit orthogonal monomer reactivity. Using this approach, copolymers can be synthesized via switching back and forth between the different active states.

The use of potentiostatic coulometry or chronoamperometry<sup>18</sup> offers specific advantages in addition to temporal control, such as tuning the extent of the electron transfer process and alleviating the need for the repeated addition of chemical redox reagents.<sup>19-20</sup> Electrochemical control of polymerization reactions has been demonstrated previously; the first example was reported in 2011 by Matyjaszewski and coworkers, who used an electric current to toggle reversibly an on/off atom transfer radical polymerization (ATRP) reaction mediated by a copper(I)/copper(II) redox couple.<sup>21</sup> Recently, electrochemically controlled polymerizations by mechanisms different than ATRP have been reported.<sup>22-27</sup> However, electrochemical control of ring-opening polymerization (ROP) has garnered less attention than that of cationic or radical polymerizations. ROP typically employs metal catalysts that offer good control and can be used to produce a wide variety of polymers, including polyesters, polyethers, and polycarbonates.<sup>28</sup>

Electrochemistry has been used to control ROP reactions either by altering monomer selectivity of a catalyst or activating a dual metal catalyst system (Figure 1). For example, Byers and coworkers reported a redox switchable ROP system using an iron precatalyst.<sup>24</sup> Oxidation and reduction toggled the selectivity of the catalyst versus specific monomers, i.e., the neutral iron species was active toward lactide (LA) polymerization, while the oxidized, cationic iron species was active toward cyclohexene oxide (CHO) polymerization (Figure 1a). The activity could be turned on or off by switching between the two oxidation states. This system only produces diblock copolymers due to catalyst limitations, and the electrochemical setup employs an intricate polymer-coated, ion selective membrane that must be fabricated prior to electrolysis.

In another example, Fors et al. reported a ferrocenyl acid that could be switched on and off for lactone (δ-valerolactone, VL, and ε-caprolactone, CL) polymerization (Figure 1b).<sup>26</sup> A decrease in pK<sub>a</sub> upon oxidation leads to activation of the monomer via protonation, and then polymerization. Propagation can be halted via reduction of the ferrocene unit that, in turn, deactivates the monomers and stops polymerization. A diblock copolymer, poly(CL-*b*-VL), could be synthesized by the sequential addition of the two monomers.

Recently, Tong and coworkers reported a Co/Zn dual catalyst system that can be activated using an electric potential toward the ROP of O-carboxyanhydrides (Figure 1c).<sup>27</sup> This work uses electrochemistry in a more involved manner than the previous examples, in that the anode helps promote the oxidative addition of a C-O bond, while the cathode acts as an electron reservoir for reductive decarboxylation. High molecular weight, isotactic polyesters

containing varying functional groups are produced in addition to stereoblock, diblock, and triblock copolymers obtained by the sequential addition of monomers.

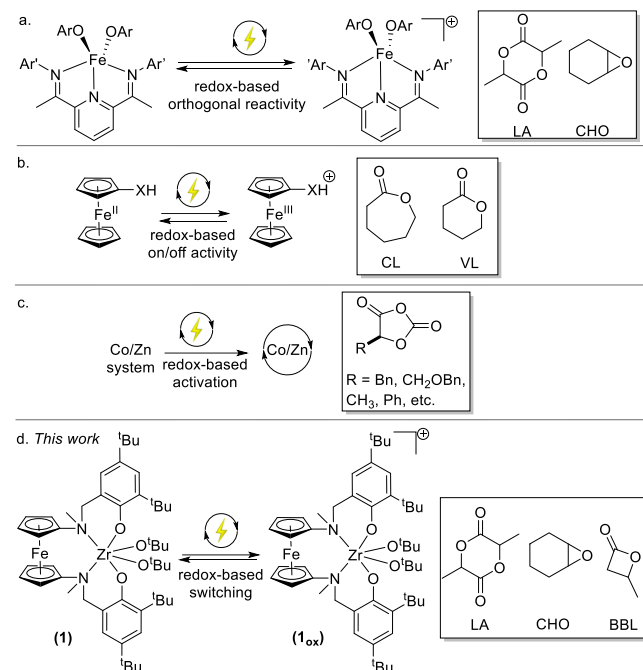


**Figure 1.** Examples of electrochemically controlled ring-opening polymerization methods with monomers used shown in boxes. a) Ring-opening polymerization of lactide and cyclohexene oxide by a redox-switchable pyridinediimine iron complex to produce diblock copolymers ( $\text{Ar} = 4\text{-methoxyphenyl}$ ;  $\text{Ar}' = 2,6\text{-dimethylphenyl}$ ). b) Electrochemical on/off control of  $\epsilon$ -caprolactone and  $\delta$ -valerolactone via a redox-based change in the pKa of a ferrocenyl acid ( $\text{X} = \text{phosphonic, (phenyl)phosphonic, or (phenyl)phosphinic acid}$ ). c) Electrochemical activation of a Co/Zn catalyst system toward O-carboxyanhydrides. d) *This work*: electrochemical system capable of producing various di-, tri-, and tetrablock copolymers of lactide,  $\beta$ -butyrolactone, and cyclohexene oxide.

Over the last decade, our group,<sup>29-46</sup> as well as others,<sup>47-57</sup> has reported metal complexes for redox switchable polymerization. We employ ferrocene based ligands as a redox handle coordinated to various metals active for the ring-opening polymerization (ROP) of cyclic ethers, esters, and carbonates. A handful of these compounds exhibit orthogonal reactivity toward various monomers in different oxidation states. For example,  $(\text{salfan})\text{Zr}(\text{O}^t\text{Bu})_2$  ( $\text{salfan} = 1,1'\text{-di}(2\text{-tert-butyl-6-N-methylmethylenephenoxy})\text{ferrocene}$ ) is active toward LA and  $\beta$ -butyrolactone (BBL) in the reduced state, and CHO in the oxidized state.<sup>42</sup> Using chemical redox reagents and a sequential addition process, we previously synthesized di- and multiblock copolymers from the aforementioned monomers. We envision that a simple electrochemical approach will allow for the one-pot synthesis of these copolymers, without the need for repeated monomer or redox reagent additions. Additionally, the system should be broadly applicable to the dozen redox-switchable metal complexes used in our group. This group of metal complexes contains both early and late

transition metals, which allow for a wider range of monomer scope.

Herein, we report an electrochemical system that maintains orthogonal reactivity and allows the formation of ABC and ABAB block copolymers (Figure 1d). This is the first time an orthogonal electrochemical switch has been used for the formation of a multiblock copolymer. Given its controlled nature, this system opens new avenues for the tailored and controlled synthesis of multiblock copolymers using a one-pot approach.

## RESULTS AND DISCUSSION

We hypothesized that a divided electrochemical cell (H-cell) with an ultrafine ( $0.9 - 1.4\ \mu\text{m}$  porosity) frit separating the working compartment (glassy carbon plate working electrode and a silver wire pseudoreference electrode) from the counter compartment (magnesium foil counter electrode) would provide sufficient separation (Figures 2, S1).<sup>22</sup> The working compartment was equipped with two small stir bars (5 and 10 mm diameter) to overcome mass transport limitations. When a bare silver wire as a pseudoreference electrode was inserted in the working compartment, experiments with tetrapropylammonium tetrakis[3,5-bis(trifluoromethyl)phenyl]borate ( $\text{TPABAr}^{\text{F}}$ ) as the supporting electrolyte and  $(\text{salfan})\text{Zr}(\text{O}^t\text{Bu})_2$  led to uncontrolled CHO polymerization, presumably by  $\text{AgBAR}^{\text{F}}$  (Figure S44). Separating the silver wire from the working compartment with a Teflon frit mostly alleviated this issue, but occasionally the silver cations that leaked into the bulk solution interfered with the desired CHO polymerization. Such initial studies substantiated the need to use an alternative electrolyte. We found that tetrapropylammonium bistriflimide ( $\text{TPANTf}_2$ , synthesis and characterization included in the SI, Figures S4-5) was innocent toward CHO and LA polymerization (Table 1, entry 1; Figure S6) even when using a bare silver wire as a pseudo-reference electrode. However, the separation of the silver pseudo-reference electrode with a Teflon frit was continuously employed for electrolysis reactions. After addressing such technical details, the cyclic voltammogram of  $(\text{salfan})\text{Zr}(\text{O}^t\text{Bu})_2$  dissolved in a 1,2-difluorobenzene solution of  $\text{TPANTf}_2$  reproducibly exhibited a reversible redox event at 360 mV versus  $\text{Ag}/\text{Ag}^+$  (Figure 2, bottom). Therefore, we chose bulk electrolysis potentials a few hundred millivolts to either side of the catalyst's redox potential ( $E_{\text{cathodic}} = 0.1\ \text{V}$  versus  $\text{Ag}/\text{Ag}^+$  and  $E_{\text{anodic}} = 0.7\ \text{V}$  versus  $\text{Ag}/\text{Ag}^+$ ) to ensure complete electron transfer to and from the catalyst.

With suitable electrolysis conditions established, the ability of this system to perform homopolymerization reactions of *L*-lactide and cyclohexene oxide was surveyed next. First, controlled reactions were carried out. The polymerizations of LA (Table S1, entry 1, Figure S8) in a 1,2-difluorobenzene solution of  $\text{TPANTf}_2$  showed that the electrolyte did not interfere with the controlled polymerization process.

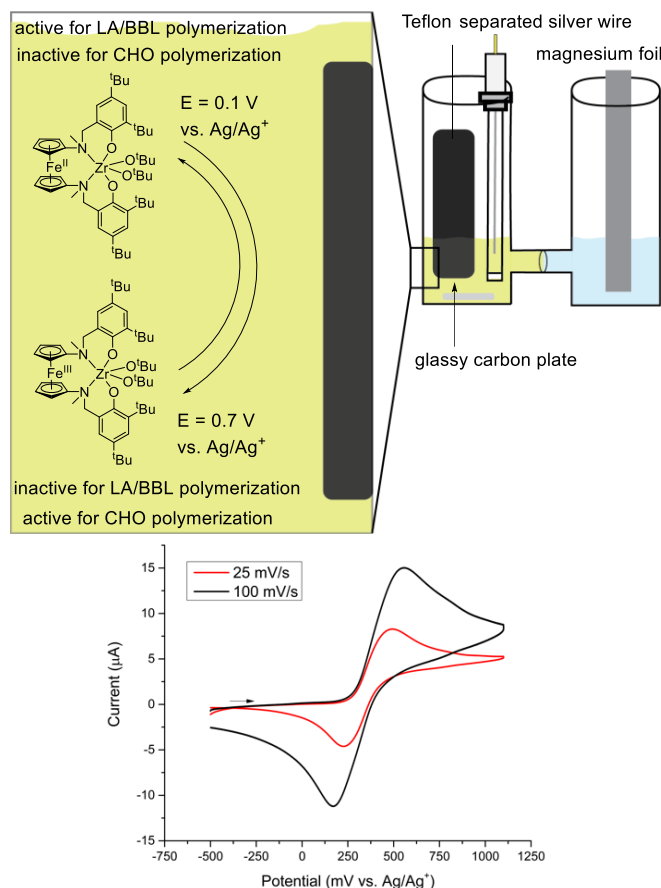


**Figure 2.** Electrochemical setup (top); inset of the general electrolysis reaction for switchable polymerization of L-lactide and cyclohexene oxide; iR corrected cyclic voltammogram of (salfan)Zr(O<sup>t</sup>Bu)<sub>2</sub> (5 mM) in 1,2-difluorobenzene with TPANTf<sub>2</sub> (75 mM) as an electrolyte (bottom).

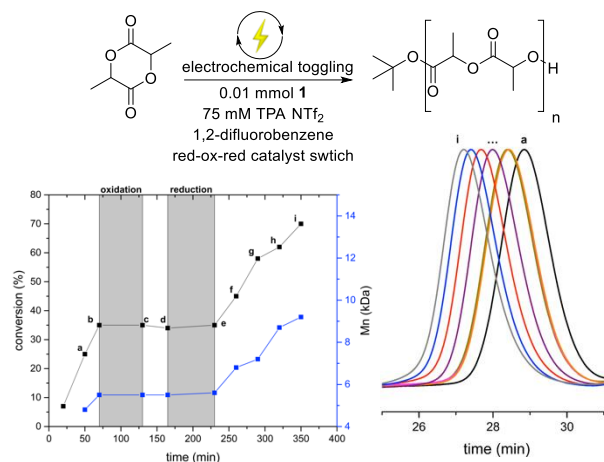


**Figure 3.** Left: control of LA polymerization mediated by an electrochemical switch of (salfan)Zr(O<sup>t</sup>Bu)<sub>2</sub>, conversion and  $M_n$  versus time of LA on/off polymerization; first gray region: electrochemical oxidation, second gray region: cathodic electrolysis. Right: SEC traces of the corresponding LA polymer aliquots. Traces b – e are nearly superimposed and only two are shown for clarity.

Next, the homopolymerization of CHO was performed. Application of an anodic potential to (salfan)Zr(O<sup>t</sup>Bu)<sub>2</sub> produced [(salfan)Zr(O<sup>t</sup>Bu)<sub>2</sub>]<sup>+</sup> (see Figures S2-3 for representative current vs. time curves) and the pale yellow solution turned brown, similar to the results obtained when using chemical oxidants. The electrochemically generated [(salfan)Zr(O<sup>t</sup>Bu)<sub>2</sub>]<sup>+</sup> is active in CHO polymerization, resulting in a polymer with a unimodal size exclusion chromatography (SEC) trace and a dispersity of 1.4 (Table S1, entry 2, Figure S9), typical of (salfan)Zr(O<sup>t</sup>Bu)<sub>2</sub>.<sup>42</sup> These results demonstrate the feasibility of using an electrochemical system for the homopolymerization of LA and CHO. Electrode washing with CH<sub>2</sub>Cl<sub>2</sub> after both anodic and cathodic electrolysis indicated very little polymer/electrolyte was deposited during the reaction (See Figures S9-10).

**Table 1.** Synthesis of various copolymers of L-lactide (LA) and cyclohexene oxide (CHO) using an electrochemical switch of (salfan)Zr(O<sup>t</sup>Bu)<sub>2</sub>.

entry	mon. 1	mon. 2	mon. 3	mon. 4	catalyst	time (h)	conv. (%) <sup>a</sup>	$M_{n, \text{exp}}^b$ (kDa)	$M_{n, \text{calc}}^c$ (kDa)	$\bar{D}$
1	LA	CHO	--	--	--	22	< 3	--	--	--
2	LA	CHO	--	--	red-ox	1.5-18	93-54	13	10	1.3
3	CHO	LA	--	--	ox-red	4-2	70-79	18	9.1	1.5
4	LA	CHO	--	--	red-ox	2-20	95-55	16	9.5	1.4
5	LA	CHO	LA	--	red-ox-red	1.5-18-2	47-70-88	15	10	1.5
6 <sup>d</sup>	LA	CHO	LA	CHO	red-ox-red-ox	0.75-16-2-24	31-25-90-57	26	24	1.3
7 <sup>e</sup>	BBL	CHO	--	--	red-ox	24-24	84-30	11	10	1.3
8 <sup>f</sup>	LA	CHO	BBL	--	red-ox-red	2-18-12	88-42-25	14	15	1.5

Conditions: 75 mM TPANTf<sub>2</sub> solution, 1.5 mL of 1,2-difluorobenzene. 0.01 mmol precatalyst, 100 equiv monomer, unless otherwise noted; LA and CHO polymerizations were carried out at 100 and 25 °C, respectively; red = (salfan)Zr(O<sup>t</sup>Bu)<sub>2</sub>; ox = (salfan)Zr(O<sup>t</sup>Bu)<sub>2</sub><sup>+</sup>; all entries were conducted using a one pot approach except entries 2, 3, and 8 which used a sequential addition

approach; [a] determined by  $^1\text{H}$  NMR spectroscopy by integrating polymer to monomer peaks and reported as total conversion of that monomer; [b] determined by SEC; [c] calculated by  $^1\text{H}$  NMR ratio of polymer to monomer peaks assuming two initiating groups; [d] 200 equiv LA and 400 equiv CHO; [e] 200 equiv each; [f] 100 equiv LA, 200 equiv CHO, 400 equiv BBL.

In order for this system to be compatible with synthesizing complex copolymers, it should impart on/off control during polymerization via an electrolysis event. Therefore, we demonstrated that during LA polymerization, an electrochemical oxidation (Figure 3, first gray region) can halt LA polymerization. During this “off” phase (Figure 3, points c to d), the conversion of LA does not change, even when heated to 100  $^\circ\text{C}$ , and the SEC traces are superimposable. These data suggest that this is a redox-based switch and not thermochemical and that electrolysis does not affect the integrity of the polymer backbone. After cathodic electrolysis (Figure 3, second gray region), LA polymerization continues, evident by increasing its conversion and polymer molecular weight, showing that bulk electrolysis had no detrimental effect on the polymer molecular weight and dispersity. Additionally, the initial rate of LA polymerization before and after the redox switch are nearly identical (See Figures S19–20).

We then set out to demonstrate a similar control over CHO polymerization. At 0.01 mmol catalyst loading, electrolysis time (roughly 45–60 mins) and polymerization time for CHO (roughly 120 mins) were too close to impart a meaningful on/off activity with any control. We lowered the catalyst loading to 0.005 mmol to decrease electrolysis time and slow down CHO polymerization. After an initial anodic electrolysis, 300 equivalents of CHO was added, reaching 18% conversion after 15 minutes. Electrochemical reduction halted CHO polymerization and, after 90 minutes, no additional CHO was polymerized. A subsequent oxidation reinitiated CHO polymerization, and resulted in a total of 62% CHO polymerization after 6 hours (Figure S18).

We propose that similar mechanistic considerations apply here as to the chemical system. Previous DFT studies investigated the nature of the redox-switchable chemoselectivity of (salan) $\text{Zr}(\text{O}^t\text{Bu})_2$  toward LA and CHO;<sup>38</sup> these studies found that LA initiation is favorable in both the reduced and oxidized state, however, LA propagation is only favorable in the reduced state. Additionally, CHO polymerization by the oxidized form of (salan) $\text{Zr}(\text{O}^t\text{Bu})_2$  was shown to favor a coordination-insertion mechanism. These mechanistic studies indicate that a single electron transfer process imparts monomer selectivity during polymerization (see Figure S43 for proposed mechanism).

With homopolymerization activity and on/off control established, we set out to synthesize various copolymers using an electrochemical switch, initially with a sequential addition approach. Diblock copolymers of LA and CHO could be readily synthesized, both starting with LA and initiating CHO incorporation via an electrochemical switch (producing pCHO-b-PLA, Table 1 entry 2; Figure S11) or via an initial anodic event to start CHO polymerization and subsequent electrochemical reduction to produce a PLA-b-pCHO copolymer (Table 1, entry 3; Figure S12). These two

copolymers exhibited a dispersity of 1.3 and 1.5, respectively (see Figures S47–48 for SEC traces), and produce similar polymers as the chemical reagent approach.<sup>42</sup> These results were encouraging and showed that we could use this technique to forge distinct blocks in a controlled fashion during polymerization.

A main objective of using the electrochemical approach was to circumvent the interference of a chemical oxidant during switchable catalysis. Previously studied oxidants either interfere with the reaction by rapidly polymerizing CHO, irreversibly oxidizing the catalyst, or leading to degradation products; in all cases, the synthesis of multiblock copolymers via a one pot approach became unattainable.<sup>42</sup> We hypothesized that this electrochemical approach could alleviate this drawback. Combining both monomers with **1** led initially to a PLA polymer; upon electrolysis, the reactivity switched from PLA to CHO incorporation. The dispersity of the resulting diblock copolymer (Table 1, entry 4; Figure S13) was 1.4, suggesting that the reaction time for CHO (16 hours) was sufficiently longer than the electrolysis time and did not prevent control over the polymerization process. Diffusion ordered spectroscopy (DOSY) was performed to confirm the synthesis of a copolymer (Figure S23); the  $^1\text{H}$  NMR peaks of the LA and CHO blocks diffused at the same rate, suggesting the two blocks were connected as a copolymer and not two homopolymers. Additionally, heteronuclear multiple bond correlation (HMBC) and heteronuclear single quantum coherence (HSQC) experiments (Figures S41 & S42) were performed on the smaller, 13 kDa diblock copolymer (Table 1, entry 2) to assign the junction units between LA and CHO blocks. A magnified  $^1\text{H}$  NMR spectrum of the isolated copolymer with proton assignments is shown in Figure 4, confirming the block copolymer nature.

Next, we looked at the feasibility of synthesizing multiblock copolymers, such as tri- or tetrablock. Using the same redox switch to make the pCHO-b-PLA diblock copolymer, followed by an additional cathodic electrolysis to reinitiate LA polymerization led to the formation of a PLA-b-pCHO-b-PLA triblock copolymer (Table 1, entry 5; Figure S14). An SEC trace of each step of the copolymer formation was taken (Figure S50) indicating the molecular weight of the copolymer increased during each block polymerization. Additionally, the DOSY data suggests that PLA and pCHO combined as one copolymer (Figure S24).

We took this one step further using three electrolysis events to make a tetrablock copolymer (Figure 5). We increased the amount of LA and CHO to 200 and 400, respectively, to ensure enough of each monomer remained for the third and fourth blocks while a polymer with a large enough molecular weight for SEC analysis was isolated.

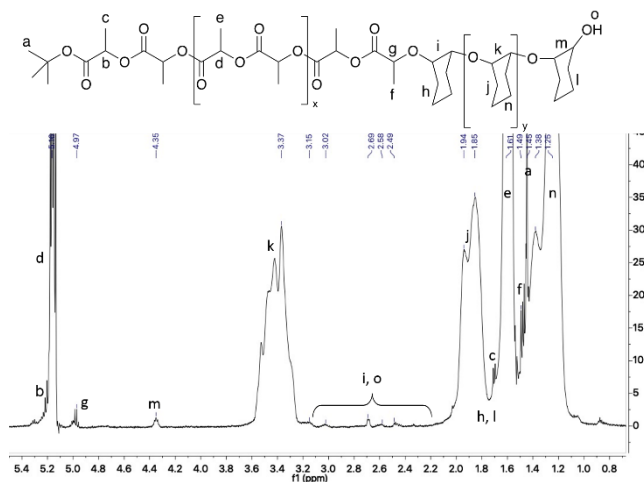


**Figure 4.** Magnified view of the  $^1\text{H}$  NMR (500 MHz,  $25^\circ\text{C}$ ,  $\text{CDCl}_3$ ) spectrum of the pCHO-b-PLA copolymer with peak assignments for bulk and junction units.

Using a reduced-oxidized-reduced-oxidized method, a pCHO-b-PLA-b-pCHO-b-PLA tetrablock copolymer (Table 1, entry 6; Figure S15) could be obtained. The final polymer molecular weight agreed with the theoretical value (26 kDa versus 24 kDa) while maintaining a relatively narrow dispersity of 1.3. The SEC trace of each step of copolymer formation and the final copolymer DOSY are shown in Figure 5 and both point to the formation of the assigned block copolymer. The  $^{13}\text{C}\{^1\text{H}\}$  NMR spectrum of the isolated copolymer is shown in Figure S36.

To expand the scope of our electrochemical system, we investigated  $\beta$ -butyrolactone (BBL) as another monomer for redox-switchable copolymerization. In the reduced state, (salfan)Zr(O<sup>t</sup>Bu)<sub>2</sub> polymerizes BBL at  $100^\circ\text{C}$ ; in the oxidized state, there is minimal activity at  $100^\circ\text{C}$  and no activity at room temperature, making it an ideal candidate for copolymerization with CHO.<sup>42</sup> Combining **1** with 200 equiv of both BBL and CHO and undergoing a red-ox catalyst switch led to the production of a pCHO-b-PHB (PHB = polyhydroxybutyrate) copolymer (Table 1, entry 7; Figure S16). The copolymer exhibited a unimodal SEC trace with a molecular weight of 11 kDa and a dispersity of 1.3 (Figure S51).

Furthermore, an ABC triblock copolymer was obtained, where LA could be polymerized first, followed by CHO and BBL using a red-ox-red switch. Because LA and BBL can be copolymerized at  $100^\circ\text{C}$  in the reduced state, a sequential addition approach was taken. Initial LA polymerization reached 88% conversion, followed by an electrochemical switch that initiated CHO incorporation. Subsequent reduction and addition of BBL initiated the third block and led to the formation of an ABC triblock copolymer (Table 1, entry 8; Figure S17). Although the final 'C' block had a smaller percent conversion of BBL monomer (25%), the final  $^1\text{H}$  and  $^{13}\text{C}$  spectra (Figures S39-40) of the isolated polymer spectra indicated its presence in the copolymer. Additionally, a unimodal SEC trace of the final copolymer (Figure S52) and DOSY (Figure S26) indicated that all  $^1\text{H}$  polymer peaks diffuse at the same rate and both suggest the formation of a triblock copolymer.

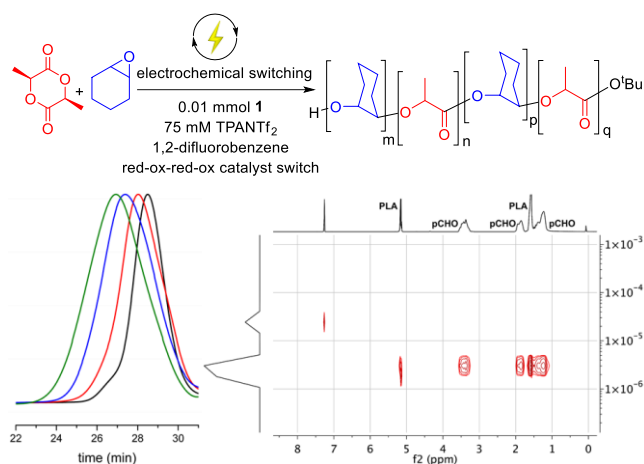


**Figure 5.** Left: SEC traces of each stage of the tetrablock copolymer formation; black: PLA, red: diblock, blue: triblock, green: tetrablock (from Table 1, entry 6, left); right: DOSY of the final tetrablock copolymer (right).

$^1\text{H}$  and  $^{13}\text{C}$  NMR spectroscopy was performed on all isolated copolymers and their assigned spectra can be found in the SI (Figures S27-40). The  $^1\text{H}$  NMR integrations were used in conjunction with the experimental molecular weights to calculate the degree of polymerization (DP, Table S2). The DP of each block is sufficiently large to describe the copolymers formed as discrete block copolymers.<sup>58</sup> Additionally, thermal gravimetric analysis (TGA) and differential scanning calorimetry (DSC) was conducted on the block copolymers synthesized to investigate their thermal properties. The TGA trace for PLA shows a  $T_{d50}$  of  $309^\circ\text{C}$  and a decomposition range of ca  $240^\circ\text{C}$  to  $350^\circ\text{C}$ , while pCHO shows a  $T_{d50}$  of  $251^\circ\text{C}$  and a decomposition range of ca  $200 - 410^\circ\text{C}$ , although with a greater initial thermal decomposition until ca  $275^\circ\text{C}$  followed by a slower decomposition until  $410^\circ\text{C}$  (Figures S53-54). The copolymers of LA and CHO (Figures S55-57) exhibit broader decomposition ranges, roughly  $225 - 340^\circ\text{C}$  for the pCHO-b-PLA diblock copolymer,  $250 - 375^\circ\text{C}$  for the PLA-b-pCHO-b-PLA triblock copolymer, and  $240 - 340^\circ\text{C}$  for the pCHO-b-PLA-b-pCHO-b-PLA tetrablock, consistent with the combined ranges for both PLA and pCHO. The pCHO-b-BBL thermal decomposition showed two steps, an initial decomposition starting around  $250^\circ\text{C}$  and the second step around  $350^\circ\text{C}$ , with a  $T_{d50}$  value of  $280^\circ\text{C}$  (Figure S58). The ABC triblock copolymer primarily decomposed in one step ranging from  $260^\circ\text{C}$  to  $340^\circ\text{C}$  with a  $T_{d50}$  of  $314^\circ\text{C}$ , but also exhibited a slower decomposition process from  $350$  to  $400^\circ\text{C}$  (Figure S59), similar to that of pCHO.

DSC analysis (Figures S60-64) shows glass transition temperatures ( $T_g$ ) of  $58^\circ\text{C}$ ,  $50^\circ\text{C}$ , and  $54^\circ\text{C}$  for the LA/CHO diblock, triblock, and tetrablock copolymers, respectively, and melting temperatures of  $\sim 154^\circ\text{C}$ . The  $T_g$  value lies on the lower end for lactide-containing polymers, which is a known phenomenon in block copolymers containing lactide.<sup>59</sup> The pCHO-b-PHB copolymer showed a  $T_g$  of  $6^\circ\text{C}$ , presumably corresponding to the PHB block, and a melting temperature of  $82^\circ\text{C}$ . Interestingly, the PHB-b-pCHO-b-PLA triblock copolymer exhibited a  $T_g$  of  $25^\circ\text{C}$  which falls



between the typical  $T_g$  of the homopolymers (5 °C for PHB,<sup>60</sup> and roughly 50–70 °C for pCHO and PLA).

## CONCLUSIONS

In summary, we report a simple electrochemical system for the redox switchable ring-opening copolymerization of L-lactide,  $\beta$ -butyrolactone, cyclohexene oxide using (salfan)Zr(O<sup>*i*</sup>Bu)<sub>2</sub> as a precatalyst. Our system was surveyed for the homopolymerization of both LA and CHO, which exhibited good control, similar to the reactions employing chemical redox reagents. Potentiostatic electrolysis could be used to toggle on/off the reactivity for LA, BBL, and CHO polymerization, and, furthermore, could switch monomer selectivity between the two monomers. A one-pot approach was used to produce diblock, triblock, and tetrablock copolymers. Using a one pot approach to produce larger tri- and tetrablock copolymers via a redox switchable approach has not been demonstrated using either chemical redox reagents or electrochemical switching. Therefore, we showed how the structure of a polymer backbone can be tuned via successive applications of an electric potential during the polymerization process. This approach also offers a unique method to control block copolymer molecular weight distributions, both by adjusting relative comonomer concentrations or slowing the electron transfer during bulk electrolysis. Lastly, because this technique is compatible with a one-pot approach, it may serve as a new method to control monomer connectivity precisely via the temporal application of an electric potential.

## ASSOCIATED CONTENT

### Supporting Information

The Supporting Information is available free of charge on the ACS Publications website.

Experimental and characterization data, NMR spectra, and SEC data (PDF)

## AUTHOR INFORMATION

### Corresponding Author

Paula L. Diaconescu — *Department of Chemistry and Biochemistry, University of California Los Angeles, Los Angeles, California 90095-1569 United States; email: pld@chem.ucla.edu*

Chong Liu — *Department of Chemistry and Biochemistry, University of California Los Angeles, Los Angeles, California 90095-1569 United States; email: chongliu@chem.ucla.edu*

### Present Addresses

<sup>§</sup> Intel Corporation, Hillsboro, OR 97124, USA

<sup>†</sup> College of Chemistry, Nankai University, Tianjin 300071, China

### Notes

The authors declare no competing financial interest.

## ACKNOWLEDGMENTS

This work was supported by the NSF (Grant CHE-180916 to PLD, CHE-2027330 to CL, and CHE-1048804 for NMR spectroscopy) and UCLA. ZCH was supported in part by an NRT-INFEWS Grant (No. DGE-1735325). We acknowledge Prof. Dunwei Wang from Boston College for the electrolyte suggestion, and Jane Yang and Prof. Heather Maynard for use of their DSC instrument.

## REFERENCES

1. Lutz, J.-F.; Ouchi, M.; Liu, D. R.; Sawamoto, M., Sequence-Controlled Polymers. *Science* **2013**, *341*, 1238149.
2. Diaz, C.; Mehrkhodavandi, P., Strategies for the synthesis of block copolymers with biodegradable polyester segments. *Polym. Chem.* **2021**, *12* (6), 783-806.
3. Lewandowski, B.; De Bo, G.; Ward, J. W.; Papmeyer, M.; Kuschel, S.; Aldegunde, M. J.; Gramlich, P. M. E.; Heckmann, D.; Goldup, S. M.; D'Souza, D. M.; Fernandes, A. E.; Leigh, D. A., Sequence-Specific Peptide Synthesis by an Artificial Small-Molecule Machine. *Science* **2013**, *339* (6116), 189-193.
4. Zhou, Y.-N.; Li, J.-J.; Wu, Y.-Y.; Luo, Z.-H., Role of External Field in Polymerization: Mechanism and Kinetics. *Chem. Rev.* **2020**, *120* (5), 2950-3048.
5. Walsh, D. J.; Hyatt, M. G.; Miller, S. A.; Guironnet, D., Recent Trends in Catalytic Polymerizations. *ACS Catal.* **2019**, *9* (12), 11153-11188.
6. Chen, G.; Xia, L.; Wang, F.; Zhang, Z.; You, Y.-Z., Recent progress in the construction of polymers with advanced chain structures via hybrid, switchable, and cascade chain-growth polymerizations. *Polym. Chem.* **2021**, *12* (26), 3740-3752.
7. Matyjaszewski, K.; Xia, J., Atom Transfer Radical Polymerization. *Chem. Rev.* **2001**, *101* (9), 2921-2990.
8. Chen, M.; Zhong, M.; Johnson, J. A., Light-Controlled Radical Polymerization: Mechanisms, Methods, and Applications. *Chem. Rev.* **2016**, *116* (17), 10167-10211.
9. Pan, X.; Tasdelen, M. A.; Laun, J.; Junkers, T.; Yagci, Y.; Matyjaszewski, K., Photomediated controlled radical polymerization. *Prog. Polym. Sci.* **2016**, *62*, 73-125.
10. Blanco, V.; Leigh, D. A.; Marcos, V., Artificial switchable catalysts. *Chem. Soc. Rev.* **2015**, *44* (15), 5341-5370.
11. Teator, A. J.; Lastovickova, D. N.; Bielawski, C. W., Switchable Polymerization Catalysts. *Chem. Rev.* **2016**, *116* (4), 1969-1992.
12. Deacy, A. C.; Gregory, G. L.; Sulley, G. S.; Chen, T. T. D.; Williams, C. K., Sequence Control from Mixtures: Switchable Polymerization Catalysis and Future Materials Applications. *J. Am. Chem. Soc.* **2021**, *143* (27), 10021-10040.
13. Leibfarth, F. A.; Mattson, K. M.; Fors, B. P.; Collins, H. A.; Hawker, C. J., External Regulation of Controlled Polymerizations. *Angew. Chem. Int. Ed.* **2013**, *52* (1), 199-210.
14. Zhao, M.; Chen, C., Accessing Multiple Catalytically Active States in Redox-Controlled Olefin Polymerization. *ACS Catal.* **2017**, *7* (11), 7490-7494.

15. Doerr, A. M.; Burroughs, J. M.; Gitter, S. R.; Yang, X.; Boydston, A. J.; Long, B. K., Advances in Polymerizations Modulated by External Stimuli. *ACS Catal.* **2020**, *10* (24), 14457-14515.
16. Lai, A.; Hern, Z. C.; Shen, Y.; Dai, R.; Diaconescu, P. L., Metal Complexes for Redox Switching and Control of Reactivity. In *Reference Module in Chemistry, Molecular Sciences and Chemical Engineering*, Elsevier: 2021.
17. Wei, J.; Diaconescu, P. L., Redox-switchable Ring-opening Polymerization with Ferrocene Derivatives. *Acc. Chem. Res.* **2019**, *52* (2), 415-424.
18. Bard, A. J.; Faulkner, L. R., *Electrochemical Methods: Fundamentals and Applications* 2nd ed.; Wiley: Hoboken, NJ, 2001.
19. Ahumada, G.; Ryu, Y.; Bielawski, C. W., Potentiostatically Controlled Olefin Metathesis. *Organometallics* **2020**, *39* (10), 1744-1750.
20. Wang, Y.; Fantin, M.; Park, S.; Gottlieb, E.; Fu, L.; Matyjaszewski, K., Electrochemically Mediated Reversible Addition-Fragmentation Chain-Transfer Polymerization. *Macromolecules* **2017**, *50* (20), 7872-7879.
21. Magenau, A. J. D.; Strandwitz, N. C.; Gennaro, A.; Matyjaszewski, K., Electrochemically Mediated Atom Transfer Radical Polymerization. *Science* **2011**, *332* (6025), 81-84.
22. Peterson, B. M.; Lin, S.; Fors, B. P., Electrochemically Controlled Cationic Polymerization of Vinyl Ethers. *J. Am. Chem. Soc.* **2018**, *140* (6), 2076-2079.
23. Qi, M.; Zhang, H.; Dong, Q.; Li, J.; Musgrave, R. A.; Zhao, Y.; Dulock, N.; Wang, D.; Byers, J. A., Electrochemically switchable polymerization from surface-anchored molecular catalysts. *Chem. Sci.* **2021**, *12*, 9042-9052.
24. Qi, M.; Dong, Q.; Wang, D.; Byers, J. A., Electrochemically Switchable Ring-Opening Polymerization of Lactide and Cyclohexene Oxide. *J. Am. Chem. Soc.* **2018**, *140* (17), 5686-5690.
25. Zhong, Y.; Feng, Q.; Wang, X.; Chen, J.; Cai, W.; Tong, R., Functionalized Polyesters via Stereoselective Electrochemical Ring-Opening Polymerization of O-Carboxyanhydrides. *ACS Macro Lett.* **2020**, *9* (8), 1114-1118.
26. Supej, M. J.; McLoughlin, E. A.; Hsu, J. H.; Fors, B. P., Reversible redox controlled acids for cationic ring-opening polymerization. *Chem. Sci.* **2021**, *12* (31), 10544-10549.
27. Wang, X.; Chin, A. L.; Zhou, J.; Wang, H.; Tong, R., Resilient Poly( $\alpha$ -hydroxy acids) with Improved Strength and Ductility via Scalable Stereosequence-Controlled Polymerization. *J. Am. Chem. Soc.* **2021**, *143* (40), 16813-16823.
28. Kremer, A. B.; Mehrkhodavandi, P., Dinuclear catalysts for the ring opening polymerization of lactide. *Coord. Chem. Rev.* **2019**, *380*, 35-57.
29. Xu, X.; Luo, G.; Hou, Z.; Diaconescu, P. L.; Luo, Y., Theoretical insight into the redox-switchable activity of group 4 metal complexes for the ring-opening polymerization of  $\epsilon$ -caprolactone. *Inorg. Chem. Front.* **2020**, *7* (4), 961-971.
30. Shen, Y.; Shepard, S. M.; Reed, C. J.; Diaconescu, P. L., Zirconium Complexes Supported by a Ferrocene-Based Ligand as Redox Switches for Hydroamination Reactions. *Chem. Commun.* **2019**, *55*, 5587-5590.
31. Lai, A.; Hern, Z. C.; Diaconescu, P. L., Switchable Ring-Opening Polymerization by a Ferrocene Supported Aluminum Complex. *ChemCatChem* **2019**, *11* (16), 4210-4218.
32. Lai, A.; Clifton, J.; Diaconescu, P. L.; Fey, N., Computational mapping of redox-switchable metal complexes based on ferrocene derivatives. *Chem. Commun.* **2019**, *55*, 7021-7024.
33. Dai, R.; Diaconescu, P. L., Investigation of a Zirconium Compound for Redox Switchable Ring Opening Polymerization. *Dalton Trans.* **2019**, *48*, 2996-3002.
34. Dai, R.; Lai, A.; Alexandrova, A. N.; Diaconescu, P. L., Geometry Change in a Series of Zirconium Compounds during Lactide Ring-Opening Polymerization. *Organometallics* **2018**, *37* (21), 4040-4047.
35. Abubekurov, M.; Wei, J.; Swartz, K. R.; Xie, Z.; Pei, Q.; Diaconescu, P. L., Preparation of multiblock copolymers via step-wise addition of l-lactide and trimethylene carbonate. *Chem. Sci.* **2018**, *9* (8), 2168-2178.
36. Abubekurov, M.; Vlček, V.; Wei, J.; Miehlich, M. E.; Quan, S. M.; Meyer, K.; Neuhauser, D.; Diaconescu, P. L., Exploring Oxidation State-Dependent Selectivity in Polymerization of Cyclic Esters and Carbonates with Zinc(II) Complexes. *iScience* **2018**, *7*, 120-131.
37. Wei, J.; Riffel, M. N.; Diaconescu, P. L., Redox Control of Aluminum Ring-Opening Polymerization: A Combined Experimental and DFT Investigation. *Macromolecules* **2017**, *50* (5), 1847-1861.
38. Quan, S. M.; Wei, J.; Diaconescu, P. L., Mechanistic Studies of Redox-Switchable Copolymerization of Lactide and Cyclohexene Oxide by a Zirconium Complex. *Organometallics* **2017**, *36* (22), 4451-4457.
39. Lowe, M. Y.; Shu, S.; Quan, S. M.; Diaconescu, P. L., Investigation of redox switchable titanium and zirconium catalysts for the ring opening polymerization of cyclic esters and epoxides. *Inorg. Chem. Front.* **2017**, *4*, 1798-1805.
40. Abubekurov, M.; Khan, S. I.; Diaconescu, P. L., Ferrocene-bis(phosphinimine) Nickel(II) and Palladium(II) Alkyl Complexes: Influence of the Fe-M (M = Ni and Pd) Interaction on Redox Activity and Olefin Coordination. *Organometallics* **2017**, *36* (22), 4394-4402.
41. Shepard, S. M.; Diaconescu, P. L., Redox-Switchable Hydroelementation of a Cobalt Complex Supported by a Ferrocene-Based Ligand. *Organometallics* **2016**, *35* (15), 2446-2453.
42. Quan, S. M.; Wang, X.; Zhang, R.; Diaconescu, P. L., Redox Switchable Copolymerization of Cyclic Esters and Epoxides by a Zirconium Complex. *Macromolecules* **2016**, *49* (18), 6768-6778.
43. Abubekurov, M.; Shepard, S. M.; Diaconescu, P. L., Switchable Polymerization of Norbornene Derivatives by a Ferrocene-Palladium(II) Heteroscorpionate Complex. *Eur. J. Inorg. Chem.* **2016**, *2016* (15-16), 2634-2640.
44. Wang, X.; Thevenon, A.; Brosmer, J. L.; Yu, I.; Khan, S. I.; Mehrkhodavandi, P.; Diaconescu, P. L., Redox Control of Group 4 Metal Ring-Opening Polymerization Activity toward l-Lactide and  $\epsilon$ -Caprolactone. *J. Am. Chem. Soc.* **2014**, *136* (32), 11264-11267.

45. Broderick, E. M.; Guo, N.; Wu, T.; Vogel, C. S.; Xu, C.; Sutter, J.; Miller, J. T.; Meyer, K.; Cantat, T.; Diaconescu, P. L., Redox control of a polymerization catalyst by changing the oxidation state of the metal center. *Chem. Commun.* **2011**, 47, 9897-9899.
46. Broderick, E. M.; Guo, N.; Vogel, C. S.; Xu, C.; Sutter, J.; Miller, J. T.; Meyer, K.; Mehrkhodavandi, P.; Diaconescu, P. L., Redox Control of a Ring-Opening Polymerization Catalyst. *J. Am. Chem. Soc.* **2011**, 133 (24), 9278-9281.
47. Delle Chiaie, K. R.; Yablon, L. M.; Biernesser, A. B.; Michalowski, G. R.; Sudyn, A. W.; Byers, J. A., Redox-triggered crosslinking of a degradable polymer. *Polym. Chem.* **2016**, 7 (28), 4675-4681.
48. Biernesser, A. B.; Delle Chiaie, K. R.; Curley, J. B.; Byers, J. A., Block Copolymerization of Lactide and an Epoxide Facilitated by a Redox Switchable Iron-Based Catalyst. *Angew. Chem. Int. Ed.* **2016**, 55 (17), 5251-5254.
49. Biernesser, A. B.; Li, B.; Byers, J. A., Redox-Controlled Polymerization of Lactide Catalyzed by Bis(imino)pyridine Iron Bis(alkoxide) Complexes. *J. Am. Chem. Soc.* **2013**, 135 (44), 16553-16560.
50. Lastovickova, D. N.; Teator, A. J.; Shao, H.; Liu, P.; Bielawski, C. W., A redox-switchable ring-closing metathesis catalyst. *Inorg. Chem. Front.* **2017**, 4 (9), 1525-1532.
51. Lastovickova, D. N.; Shao, H.; Lu, G.; Liu, P.; Bielawski, C. W., A Ring-Opening Metathesis Polymerization Catalyst That Exhibits Redox-Switchable Monomer Selectivities. *Chem. Eur. J.* **2017**, 23 (25), 5994-6000.
52. Varnado, C. D.; Jr; Rosen, E. L.; Collins, M. S.; Lynch, V. M.; Bielawski, C. W., Synthesis and study of olefin metathesis catalysts supported by redox-switchable diaminocarbene[3]ferrocenophanes. *Dalton Trans.* **2013**, 42 (36), 13251-13264.
53. Arumugam, K.; Varnado, C. D.; Sproules, S.; Lynch, V. M.; Bielawski, C. W., Redox-Switchable Ring-Closing Metathesis: Catalyst Design, Synthesis, and Study. *Chem. Eur. J.* **2013**, 19 (33), 10866-10875.
54. Tennyson, A. G.; Lynch, V. M.; Bielawski, C. W., Arrested Catalysis: Controlling Kumada Coupling Activity via a Redox-Active N-Heterocyclic Carbene. *J. Am. Chem. Soc.* **2010**, 132 (27), 9420-9429.
55. Chen, C., Designing catalysts for olefin polymerization and copolymerization: beyond electronic and steric tuning. *Nat. Rev. Chem.* **2018**, 2 (5), 6-14.
56. Zou, W.; Pang, W.; Chen, C., Redox control in palladium catalyzed norbornene and alkyne polymerization. *Inorg. Chem. Front.* **2017**, 4 (5), 795-800.
57. Chen, M.; Yang, B.; Chen, C., Redox-Controlled Olefin (Co)Polymerization Catalyzed by Ferrocene-Bridged Phosphine-Sulfonate Palladium Complexes. *Angew. Chem. Int. Ed.* **2015**, 54 (51), 15520-15524.
58. Gody, G.; Zetterlund, P. B.; Perrier, S.; Harrisson, S., The limits of precision monomer placement in chain growth polymerization. *Nat. Commun.* **2016**, 7 (1), 10514.
59. Nagarajan, S.; Deepthi, K.; Gowd, E. B., Structural evolution of poly(l-lactide) block upon heating of the glassy ABA triblock copolymers containing poly(l-lactide) A blocks. *Polymer* **2016**, 105, 422-430.
60. Czerniecka-Kubicka, A.; Frącz, W.; Jasierski, M.; Błazejewski, W.; Pilch-Pitera, B.; Pyda, M.; Zarzyka, I., Thermal properties of poly(3-hydroxybutyrate) modified by nanoclay. *J. Therm. Anal. Calorim.* **2017**, 128 (3), 1513-1526.



